Cell Reports, Volume *34*

Supplemental Information

RAD52 Adjusts Repair of Single-Strand Breaks via Reducing DNA-Damage-Promoted XRCC1/LIG3α Co-localization

Jian Wang, You-Take Oh, Zhentian Li, Juan Dou, Siyuan Tang, Xiang Wang, Hongyan Wang, Shunichi Takeda, and Ya Wang

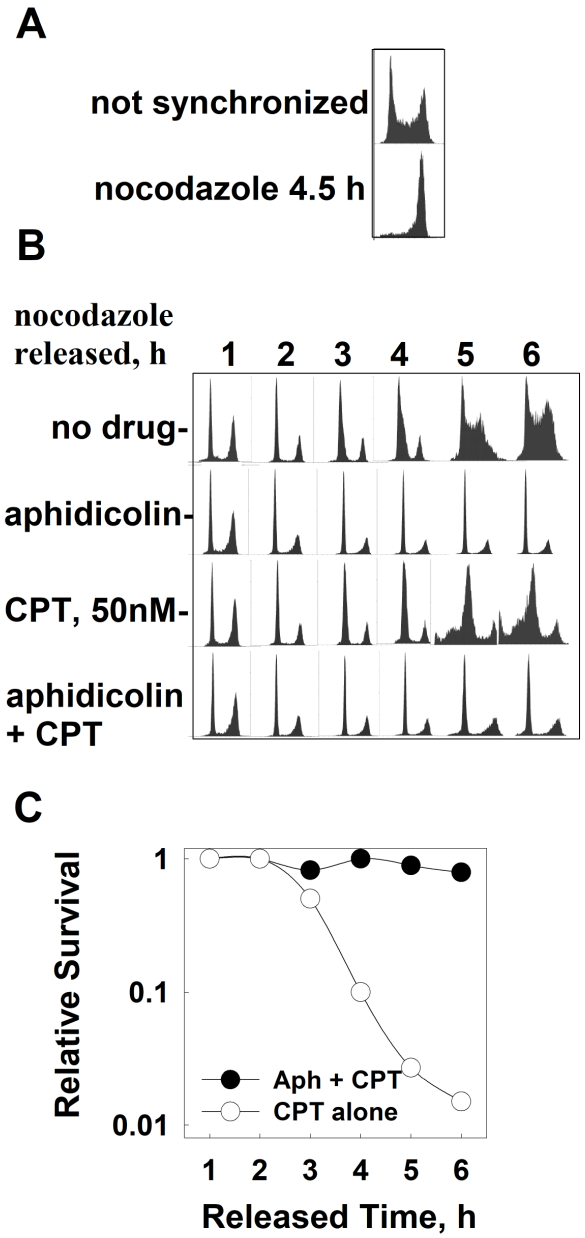

Figure S1. Related to Figure 1. Preventing cells from entering S phase abolishes their sensitivity to CPT. (A) Cell cycle distribution of WT DT40 cells treated with nocodazole (0.4 μg/mL) for 4.5 h was analyzed using a flow cytometer. (B) Cell cycle distribution 1-6 h after nocodazole release. At time zero, aphidicolin (2.5 μg /mL) and/or CPT (50 nM) was added to the cell culture. (C) Cell survival with or without aphidicolin treatment was measured using clonogenic assays as described in our previous publication (Wang et al., 2010).

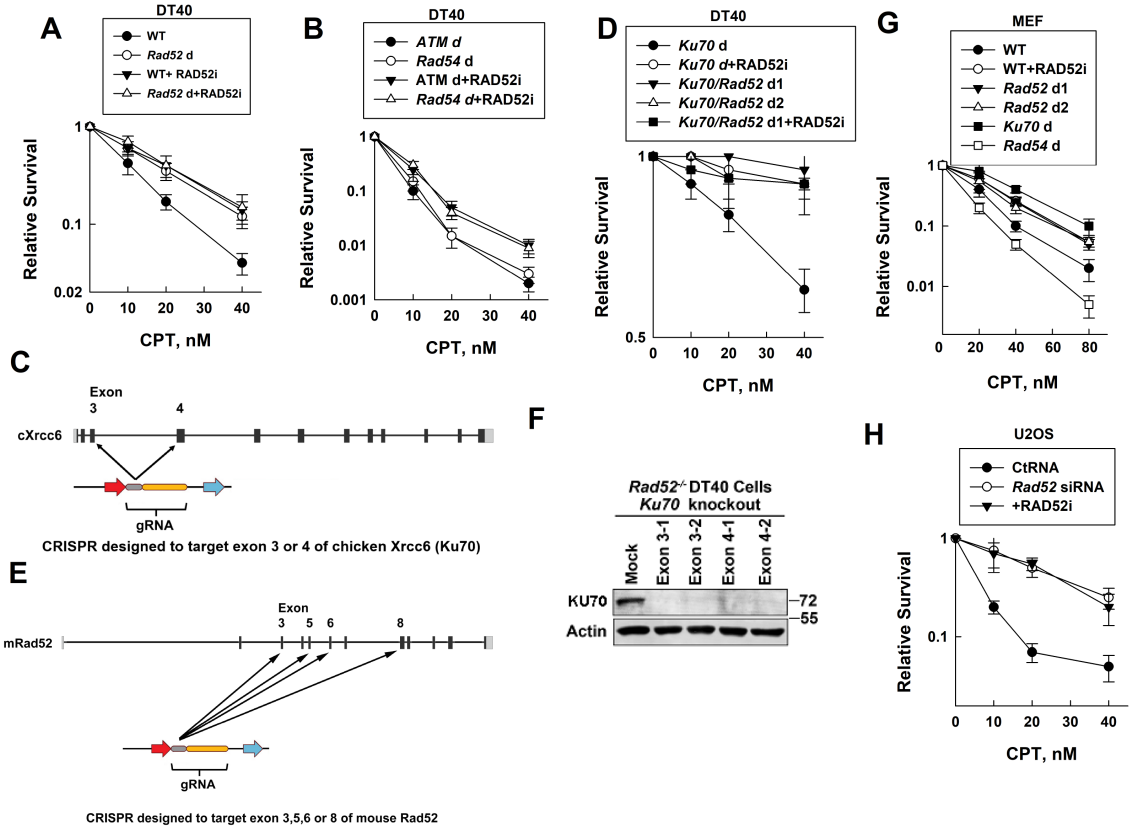

Figure S2. Related to Figure 1. RAD52 promotes CPT-induced vertebrate/mammalian cells killing. (A) WT and *Rad52*$^{-/-}$(*Rad52* d) DT40 cell sensitivities to CPT were measured using the CellTiter-Glo® Luminescent Cell Viability Assay Kit following our modified protocol as described in the Methods and confirmed by clonogenic assay. RAD52i (2.5 μM), was added to cell cultures 1.5 h before adding different concentrations of CPT. The data were analyzed from three independent experiments. (B) Similar CPT sensitivity assays were performed using *Rad54*$^{-/-}$ (*Rad54* d) or *Atm*$^{-/-}$ (*Atm* d) DT40 cells. (C) Strategy for knocking out *Ku70* from *Rad52*-deficient DT40 cells using CRISPR/Cas9. (D) *Ku70*-deficient (*Ku70* d) and *Rad52/Ku70* double knockout (*Rad52/Ku70* d1 targeting exon 3-1; *Rad52/Ku70* d2 targeting exon 4-1) DT40 cell sensitivities to CPT with or without RAD52i. Data: mean ± SEM from three independent experiments. (E) Strategy for knocking out *Rad52* from WT MEFs by using CRISPR/Cas9. (F) KU70 levels were detected by western blotting in WT or *Rad52/Ku70* double knockout DT40 cell lines generated using CRISPR/Cas9 (2 from targeting exon 3 and 2 from targeting exon 4). The labels at right indicate protein molecular weight (kDa). (G) WT, RAD52i-treated, *Rad52*-deficient (*Rad52* d1 targeting exon 3-1; *Rad52* d2 targeting exon 3-2), *Ku70*-deficient (*Ku70* d) and *Rad54*-deficient (*Rad54* d) MEF sensitivities to CPT using a clonogenic assay. Data: mean ± SEM from three independent experiments. (H) U2OS cell sensitivity to CPT after treatment with control RNA (Ct RNA), *Rad52* siRNA or RAD52i. Data: mean ± SEM from three independent experiments.

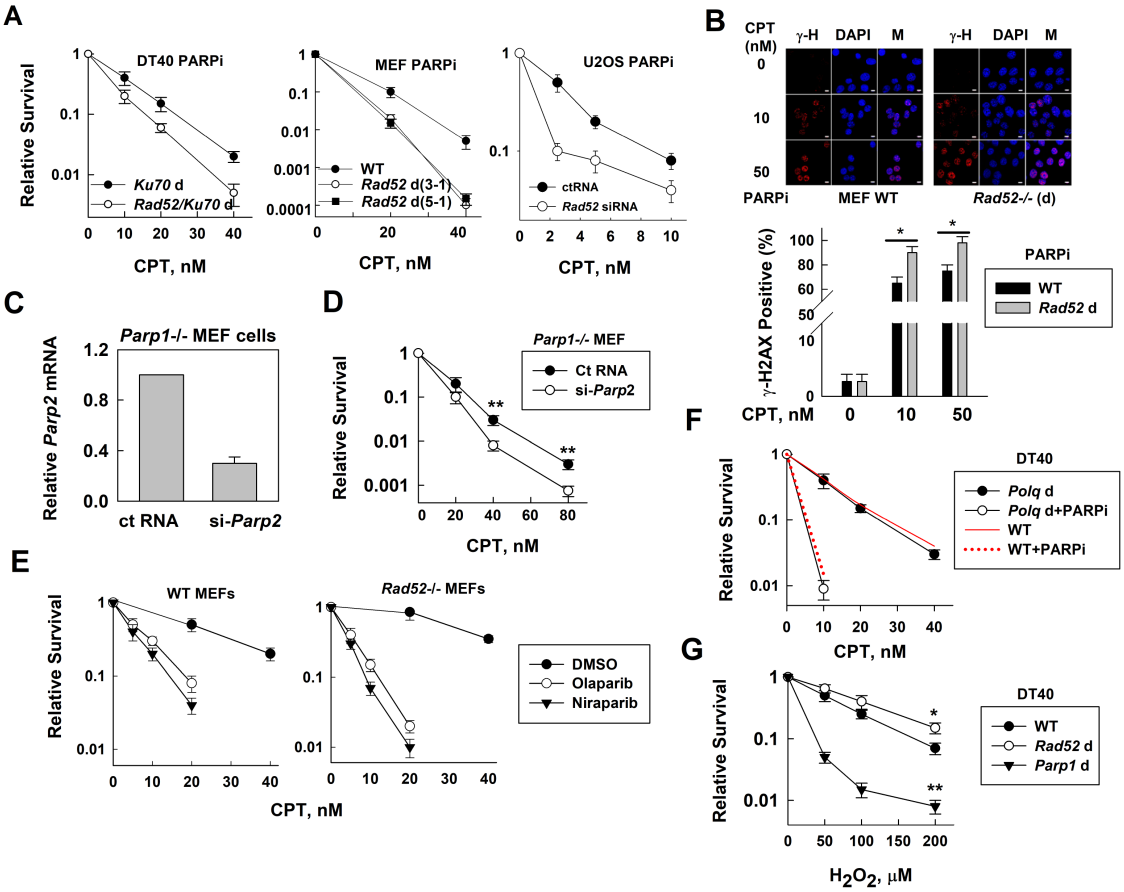

Figure S3. Related to Figure 2. RAD52 suppresses PARP-mediated repair of CPT-induced SSBs. (A) (Left) *Ku70*$^{-/-}$ or *Ku70/Parp1* double knockout (*Ku70/Rad52* d) DT40 cell sensitivities to CPT with or without PARPi (olaparib, 1 μM for 1.5 h before CPT treatment). Error bars, s.e.m. The data were analyzed from three independent experiments. (Middle) WT, *Rad52* d1 (R52-1), or *Rad52* d2 (R52-2) MEF sensitivities to CPT with or without PARPi. Data: mean ± SEM from three independent experiments. (Right) U2OS cell sensitivities to CPT after treatment with Ct RNA or *Rad52* siRNA with or without PARPi. Data: mean ± SEM from three independent experiments. (B) Top, images of CPT-induced γ-H2AX foci. WT or *Rad52*$^{-/-}$ MEFs were treated with PARPi (olaparib, 1 μM for 1.5 h), and then exposed to different concentrations of CPT for 30 min. The cells were collected for immunostaining with an anti-γ-H2AX antibody and counterstained with DAPI (scale bar = 8 μm). Bottom, percentage of cells with γ-H2AX foci (n = 50 cells). Similar results were observed from two clones of *Rad52*-deficient cells. Data: mean ± SEM. * $P < 0.05$. (C) *Parp2* mRNA levels were measured for evaluating the siRNA knock-down efficiency by real-time PCR with primers listed in key resources table. (D) CPT sensitivities were measured in *Parp1*-deficient MEFs treated with control or *Parp2* siRNA for 24 h, then with CPT for an additional 24 h. Data: mean ± SEM of three independent experiments. **, $P \leq 0.01$. (E) WT and *Rad52*-deficient MEFs were treated with DMSO or PARPi (1 μM olaparib or niraparib) for 1.5 h and then treated with different concentrations of CPT for 24 h. The survival results were obtained using the clonogenic assay described in the Methods. Data: mean ± SEM from three independent experiments. (F) Sensitivity of WT or *Polq*-deficient (*Polq* d) DT40 cells to CPT was measured with or without PARPi. The data were analyzed from three independent experiments. (G) WT, *Rad52*- deficient or *Parp1*-deficient (*Parp1* d) DT40 cells were centrifuged at room temperature (0.5 x g, 2 min), washed by warm PBS and suspended in PBS. Cells were exposed to different concentrations of H_2O_2 at room temperature for 30 min, washed with PBS, added to fresh culture medium, and culturing continued for 3 days. Cell survival was then measured. Data: mean ± SEM from three independent experiments, *$P \leq 0.05$; **$P \leq 0.001$.

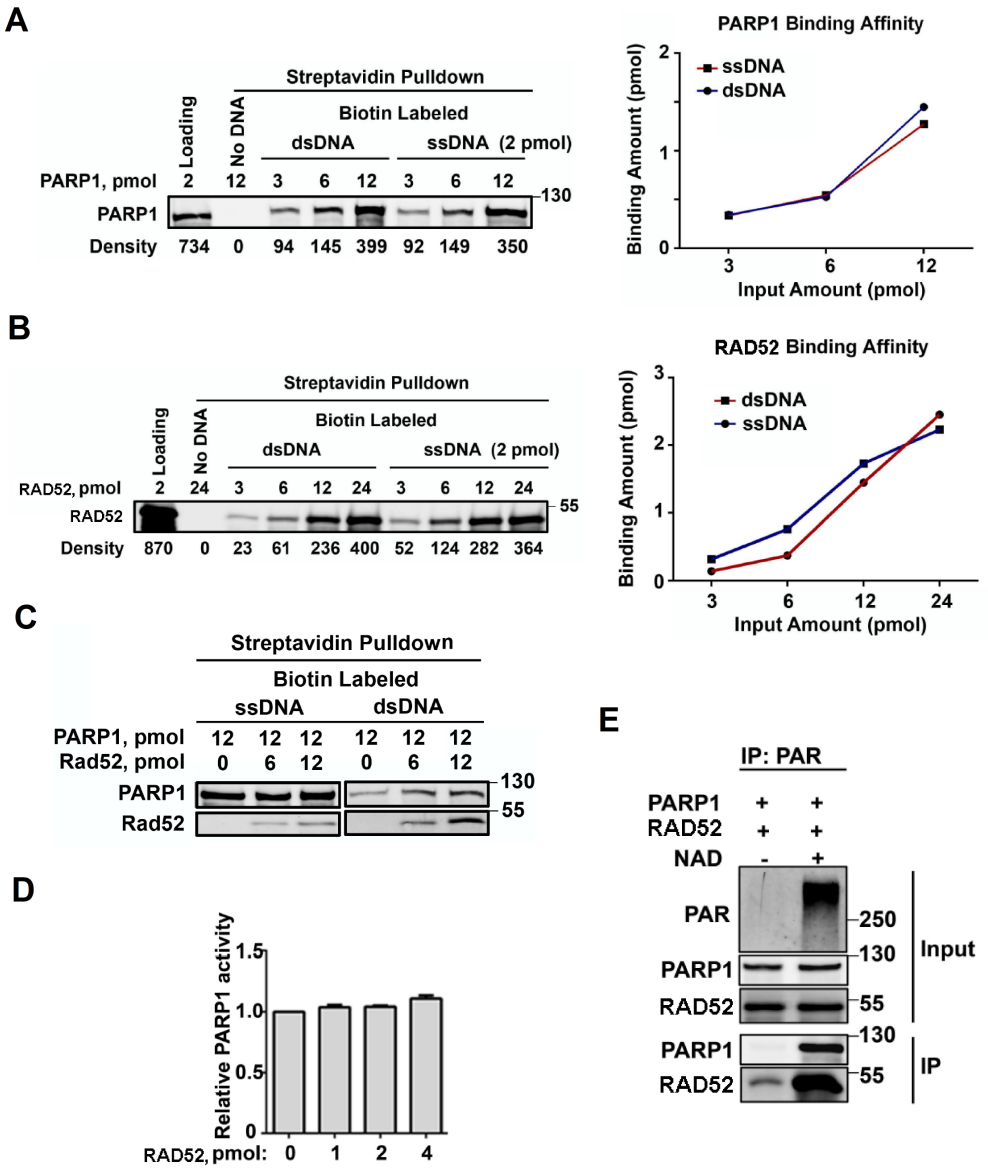

Figure S4. Related to Figure 2. RAD52 does not affect PARP1 DNA binding affinity and PARP activity. (A) Left, purified PARP1 protein was incubated with biotin labeled ssDNA or dsDNA for 30 min, then streptavidin pulldown products were evaluated by western blotting using a PARP1 antibody. Right, graphic representation of relative DNA binding affinity of PARP1 based on the data in the left panel. (B) Left, purified RAD52 protein was incubated with biotin labeled ssDNA or dsDNA for 30 min, then streptavidin pulldown products were evaluated by western blotting using a RAD52 antibody. Right, graphic representation of relative DNA binding affinity of RAD52 based on the data in the left panel. (C) Streptavidin pulldown of biotin-labeled ssDNA or dsDNA bund to PARP1 and RAD52 proteins mixed at the indicated amounts. Proteins were evaluated by western blotting. (D) *In vitro* PARP1 activity after adding the indicated amounts of RAD52 protein. (E) IP of PARP1 and RAD52 proteins from the *in vitro* pADP-ribosylation reaction using a PAR antibody was evaluated by western blotting.

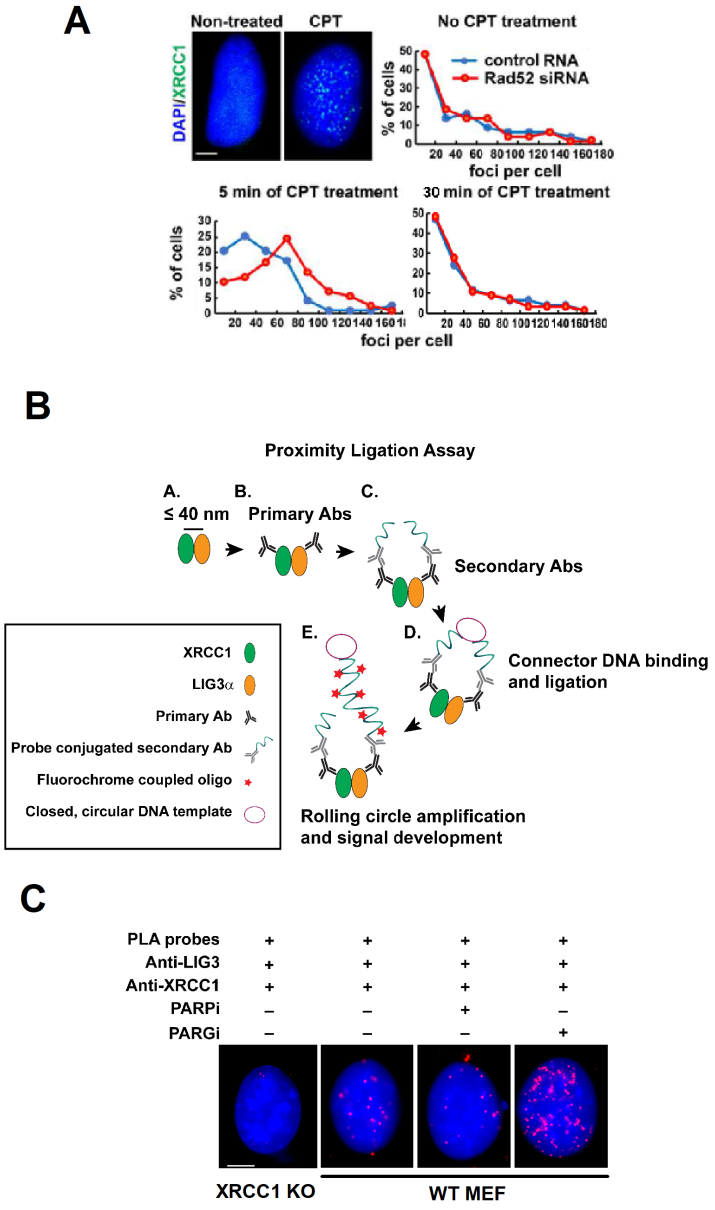

Figure S5. Related to Figure 3. RAD52 suppresses XRCC1/LIG3α co-localization in CPT-treated cells. (A) XRCC1 foci were detected in U2OS cells transfected with control or *Rad52* siRNA, followed with 10 nM CPT treatment, and then fixed and stained with an anti-XRCC1 antibody. Images at left show XRCC1 foci formed after CPT treatment (scale bar = 5 μM). The plots at right show the percentage of cells with a given number of XRCC1 foci per cell at 5 or 30 min after CPT treatment. Cells from 5 to 6 randomly selected fields (n = 50 cells) in each group were quantified using ImageJ. (B) Schematic illustration of the proximity ligation assay (PLA). A) Interacting XRCC1 and LIG3α are within close proximity (≤ 40 nm). B) Mouse anti-XRCC1 and rabbit anti-LIG3α primary antibodies bind to their targets. C) The PLA probes (oligonucleotides conjugated to donkey anti-mouse and donkey anti-rabbit secondary antibody) then bind to respected primary antibody to form complexes. D) Connector DNA is hybridized to probes in close proximity, then ligated to a circle. E) Rolling circle amplification generates substrates that were then hybridized to fluorochromes coupled oligonucleotides to allow detection using fluorescence microscopy. (C) The image of XRCC1/LIG3α foci in *Xrcc1*-deficient MEFs (as a negative control) or WT MEFs treated with or without PARPi or PARGi for 1.5 h fixed for PLA (scale bar = 5 μM).

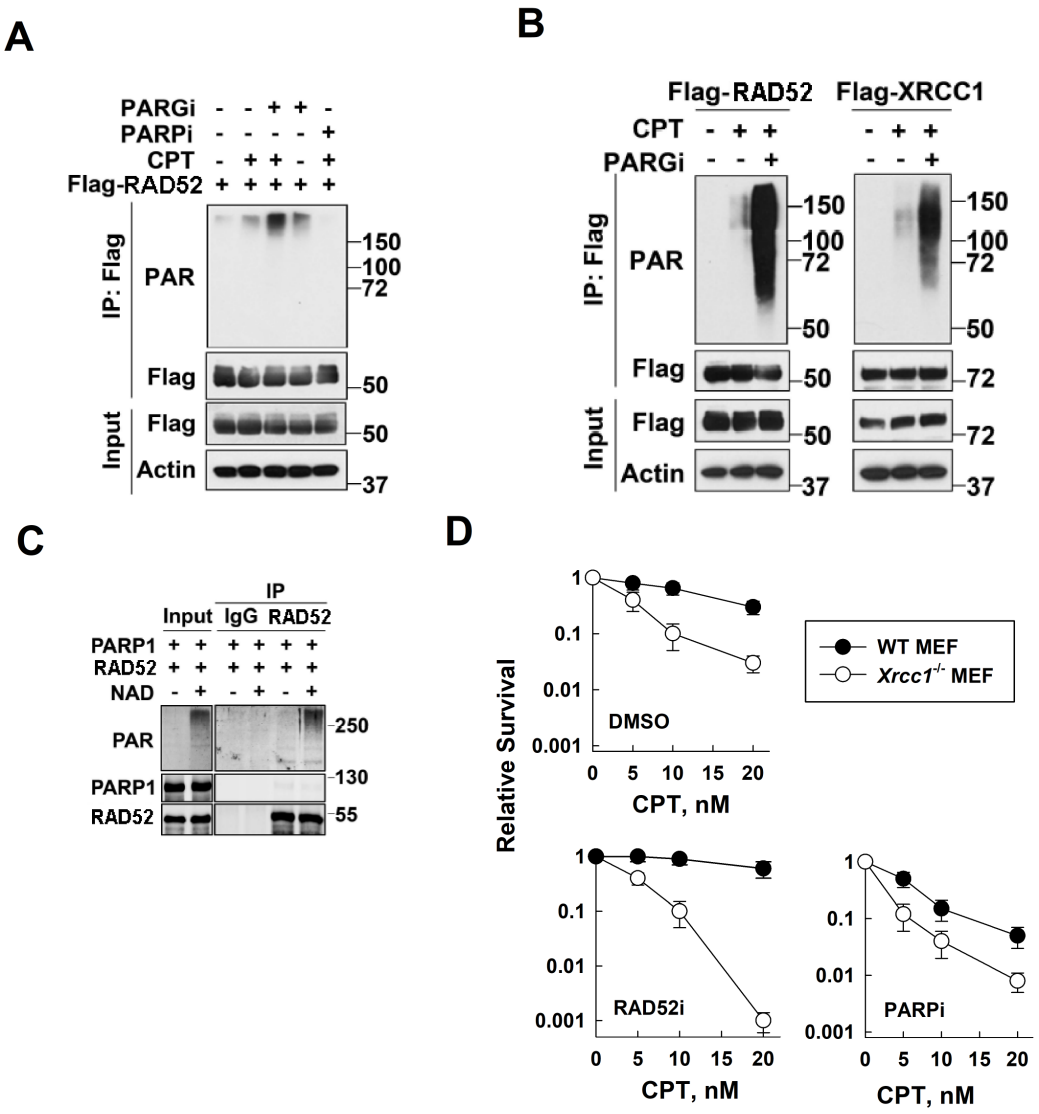

Figure S6. Related to Figure 3. RAD52 suppresses XRCC1 function in DNA damaged cells. (A) HEK293T cells were transfected with Flag-tagged *Rad52* for 24 h and then treated with PARPi for 1.5 h followed by 20 nM CPT for 12 h. The cells were treated with a PARG inhibitor (PARGi) for an additional 1 h. The PAR antibody was used to detect the IP sample. The cell lysates were subjected to IP with Flag antibody and evaluated by western blotting. (B) HEK293T cells were transfected with Flag-tagged *Rad52* or *Xrcc1* for 24 h, then treated with 20 nM CPT for 12 h. Cells were treated with a PARGi for an additional 1 h. The PAR antibody was used to detect the IP sample. The cell lysates were subjected to IP with a Flag antibody and evaluated by western blotting. (C) IP of PARP1 and RAD52 proteins after an *in vitro* PARylation reaction using an IgG or RAD52 antibody was evaluated by western blotting for PAR. (D) WT and *Xrcc1*-deficient MEFs were treated with DMSO, RAD52i or PARPi for 1.5 h, then treated with different concentrations of CPT for 24 h. The survival results were obtained using the clonogenic assay described in the Methods. Data: mean ± SEM from three independent experiments.

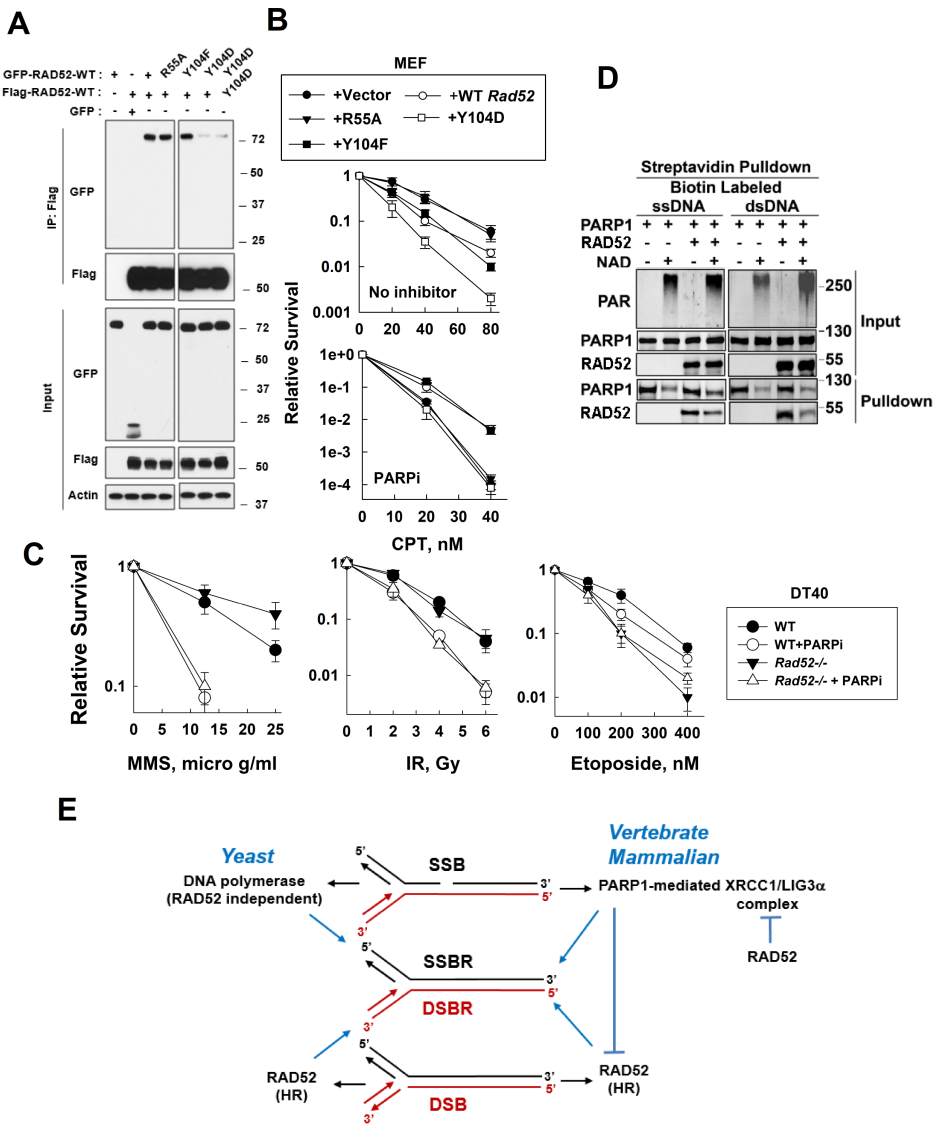

Figure S7. Related to Figure 4. A strategy to enhance the inhibitory effects of RAD52 on SSBR and sensitize cells to different DNA damaging agents. (A) HEK293T cells were co-transfected with Flag-tagged and GFP-tagged WT or mutant *Rad52*. After 36 h after transfection, whole-cell protein lysates were prepared from these cells for the assessment of RAD52 oligomerization via IP. (B) Top, sensitivity of MEF cells expressing vector, WT, or mutant *Rad52* (R55A, Y104D or Y104F) to CPT without PARPi. Bottom, sensitivity of MEF cells expressing vector, WT or mutant *Rad52* (R55A, Y104D or Y104F) expressing cell sensitivity to CPT with PARPi. Data: mean ± SEM from three independent experiments. (C) WT or *Rad52*-deficient DT40 cells were treated with different DNA damage inducers including ionizing radiation (IR), methyl methanesulfonate (MMS) and etoposide (Top II inhibitor) for 6 doubling times and the survival experiments were performed using the kit described in the Methods (confirmed by clonogenic assays). Data: mean ± SEM ofrom three independent experiments. (D) Streptavidin pulldown of PARP1 and RAD52 proteins (12 pMol) after the *in vitro* PARylation reaction and incubation with biotin-labeled ssDNA or dsDNA evaluated by western blotting. (E) A model describes the major different effects of RAD52 on SSBR between yeast (left), and vertebrate/mammalian cells (right). SSBs are mainly repaired by DNA polymerase in yeast, which is independent of RAD52. However, SSBR is dependent on PARP1/XRCC1/LIG3α–mediated pathways in vertebrate/mammalian cells, which prevents DSB generation. In addition, the HR pathway (including RAD51, BRCA1/2 and RAD52, etc.) is adjusted/limited by PARylation in vertebrate/mammals.

Table S1. Related to Figure 4. Primers for mutant m*Rad52*

Mutation of m*Rad52*		
R55A	**F**	5'-AGACTGGGTCCAGAGTACATTAGCAGCGCCATGGCTGGAGGAGGTCAGAAGGTG -3'
	R	5'-CACCTTCTGACCTCCTCCAGCCATGGCGCTGCTAATGTACTCTGGACCCAGTCT-3'
Y104F	**F**	5'-GATTTTGTTGACCTCAACAATGGCAAGTTCTTCGTGGGAGTCTGTGCATTTGTAAAGGTG-3'
	R	5'-CACCTTTACAAATGCACAGACTCCCACGAAGAACTTGCCATTGTTGAGGTCAACAAAATC-3'
Y104D	**F**	5'- GATTTTGTTGACCTCAACAATGGCAAGTTCGACGTGGGAGTCTGTGCATTTGTAAAGGTG-3'
	R	5'-CACCTTTACAAATGCACAGACTCCCACGTCGAACTTGCCATTGTTGAGGTCAACAAAATC-3'